28TH INTERNATIONAL POWER SYSTEM CONFERENCE 4-6 NOV. 2013 TEHRAN-IRAN
بیست و هشتمین کنفرانس بین المللی برق
No. E-13-AAA-0000

Dynamic Analysis and Interactions of Hybrid Electric Vehicle with Batteries, Ultracapacitors and Fuel Cell

Mahdi Rajabzadeh, Seyed Mohammad Taghi bathaee, Masoud Aliakbar Golkar
Faculty of Electrical and Computer Engineering
K. N. Toosi University of Technology
Tehran, Iran
rajabzzadeh@yahoo.com, bathaee@kntu.ac.ir, golkar@eetd.kntu.ac.ir

***Abstract*—This paper studies the impact of fuel-cell (FC) performance and control strategies on the benefits of hybridization. One of the main weak points of the FC is slow dynamics dominated by a temperature and fuel-delivery system. Although many researchers have investigated the use of different powertrain topologies, component sizes, and control strategies in fuel cell vehicles, a detailed parametric study of the vehicle types must be conducted before a fair comparison of fuel-cell vehicle types can be performed. In this paper, a dynamic model of a hybrid electric vehicle that includes fuel cells, batteries, ultracapacitors, and induction machine drives is presented. Simulation results of vehicle configuration are discussed. The focus of the model is a detailed assessment of different subsystem components.**

Keywords—Dynamic hybrid electric vehicle model; Ultracapacitor model; Battery model; Fuel Cell model and hybrid electric vehicle configuration

I. INTRODUCTION

In hybrid topologies, since the vehicle is no longer dependent on only one type of fuel, they have many benefits for the vehicle, from emission reduction to performance and efficiency improvements. The efficiency and all-electric range of hybrid electric vehicles (HEVs) depend on the capability of their energy-storage system (ESS), which not only is utilized to store large amounts of energy but also should be able to release it quickly according to load demands [1-2].

In advanced automotive systems such as hybrid electric vehicles, electric vehicles (EVs), and fuel cell vehicles (FCVs), electrical power is utilized to drive automotive subsystems [3], [4]. Recent advances in the areas of power electronics, electric motor drives, control electronics, and digital signal processors are already providing the impetus to improve the performance of automotive electrical systems and their reliability [5].

Energy storage, whether battery or ultracapacitor, can be employed to reduce the cost and improve the performance of a hybrid electric vehicle (HEV). The voltage level and dynamic characteristic of the energy storage components are normally different from the primary energy sources, and a power converter needs to be incorporated into the entire vehicle energy management system [6]–[9]. Sizing energy storage and controlling energy flow are the keys to achieving better fuel efficiency.

Fuel Cells (FCs) are able to generate electrical power with high efficiency, low operation noise, and no emissions from hydrogen gaze and air. Polymer electrolyte membrane (or proton exchange membrane) FCs (PEMFCs) utilize a solid polymer electrolyte membrane, operate at lower temperature, and are considered by many to be the most suitable for vehicle applications such as cars, buses, tramways, trains, or aircraft [10], [11].

A lot of work has been done to investigate optimal sizing and control strategies for fuel-cell–battery [12], [13], [16], [17], fuel-cell–ultracapacitor [12]-[15], and fuel-cell– battery–ultracapacitor [18], [19] vehicles. Most studies implement a coarse parametric search on the component sizes and some also vary the control parameters. To ensure optimality, the control and plant parameters should be varied simultaneously due to plant–controller coupling [20]. Other deficiencies include not using a detailed model of the dc/dc converter(s) and not including cost in the analysis, although cost is a major obstacle for fuel cell vehicles [21].

In this paper, a dynamic model for a HEV with fuel cell, battery and ultracapacitor is developed and analyzed. It is validated by simulation results and will provide a significant contribution to the field of the multisource system, particularly in nonlinear power electronics applications. In Section II, the hybrid energy storage systems for vehicular application are presented in detail. The dynamic system and subsystem modeling will be explained in detail in Section III. The simulation results and long term analysis for various conditions are presented in Section IV. Simulation results will show the system performance during load cycles.

II. HYBRID ENERGY-STORAGE SYSTEMS FOR VEHICULAR APPLICATIONS

The energy storage system (ESS) of most of the commercially available HEVs is composed of only battery packs with a bidirectional converter connected to the high-voltage dc bus. Topologies to hybridize ESSs for FC hybrid vehicles (FCHVs) have been developed to improve miles per gallon efficiency. Various topologies can be introduced by combining energy sources with different characteristics. Most of these combinations share one common feature, which is to efficiently combine fast response devices with high power density and slow response components with high energy density. For battery/UC systems, bidirectional dc/dc

Identify applicable sponsor/s here. If no sponsors, delete this text box (*sponsors).*

converters are widely used to manage power flow directions, either from the source to the load side for acceleration or from the load side to sources during regenerating periods. [22].

A. Structure of the Hybrid Power Sources

Different power converter topologies can be used for the power electronic interface between the FC and the utility dc bus. For the dc link voltage level, it depends on its applications.

Basically, low-voltage high-current structures are needed because of FC electrical characteristics. A classical boost converter is often selected because it can be operated in the current control mode in a continuous condition mode. However, a classical boost converter will be limited when the power increases or for higher step-up ratios [28].

One may summarize here again that the constraints to operate an FC are as follows.

a) The FC power or current must be kept within an interval (a rated value, a minimum value, or zero).

b) The FC current must be controlled as a unidirectional current.

c) The FC current slope must be limited to the maximum absolute value (e.g., 4 A ·s1) to prevent an FC stack from the fuel starvation phenomenon.

d) The switching frequency of the FC current must be greater than 1.25 kHz and the FC ripple current must be lower than around 5% of the rated value to ensure minor impact to the FC conditions [29].

The Proposed structure of FC/Battery/Ultracapacitor Hybrid Power Sources is shown in Fig. 1. The battery actual voltage curve is not constant. It is linear over most of its operating range. The battery voltage variation is at least 25%. Nonetheless, at the end of discharge, the battery voltage decreases very rapidly toward zero. This is because the internal resistance of a lead-acid battery is almost linear during discharge, but the losses are largely below 25% SOC due to the increase in the internal resistance of the battery. There is no battery converter in this structure to improve system efficiency and converter cost. Then, this system will be operated based on unregulated dc bus voltage, in which the dc bus voltage is equal to the battery voltage. The ultracapacitor module is frequently connected to the dc bus by means of a bidirectional dc/dc converter [30] and [31]. Ultracapacitor current, which flows across the storage device, can be positive or negative, allowing energy to be transferred in both directions.

B. Energy Management of the Hybrid Power Sources

Energy management in hybrid vehicles can be used to store energy generated at one operating load and then supplement the propulsion requirements at a different load condition (i.e., load leveling). Energy that is processed through the power converters and storage systems always has losses associated with it. Thus, a hybrid electric energy management system can only improve the overall fuel efficiency of a vehicle by shifting the operation of the fuel converter to an improved efficiency load condition by an amount sufficient to offset the losses of the energy storage and discharge processes. Key features of energy management power converters are: 1) high-power dc to dc and 2) bidirectional power flow.

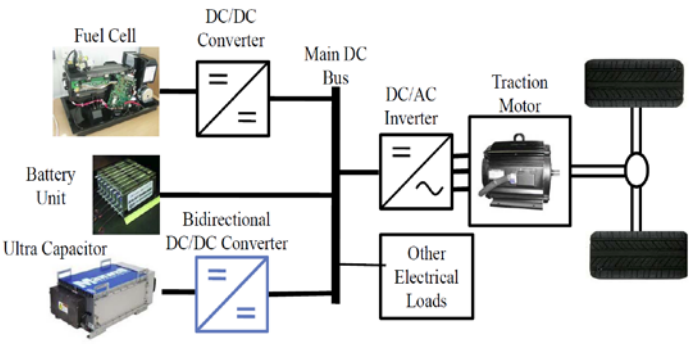

Fig. 1. Proposed structure of FC/Battery/Ultracapacitor Hybrid Power Sources

Bidirectional power flow enables the energy capture of regenerative brake and energy release during startup and hill climbing. The regenerative brake energy is always desirable no matter how high the losses are, as this energy would otherwise be dissipated and lost as heat in the friction brakes. Efficient energy management power conversion and storage for regenerative braking is of course desirable and leads to improved fuel efficiency for transient drive cycles [32].

When a FC operates, its fuel (hydrogen and oxygen) flows are controlled by an "FC controller," which receives current demand. The fuel flows must be adjusted to match the reactant delivery rate to the usage rate by the FC controller [33].

The problem of conventional control strategies is well known: The definition of system states (state-machine-used) implies control algorithm permutations that may lead to a phenomenon of chattering when the system is operating near a border between two states. The control algorithm presented here is not based on the state definition; therefore, naturally, it does not present the problem of chattering near state borders.

III. System and Subsystem Modeling

The dynamic model of an HEV system has been implemented in the Matlab/Simulink environment. Advantages of Matlab are the extensive component library of Simulink, the flexibility in implementing behavioral and physical models, Simulink's modular interface with subsystems, and simple data handling and storage.

A. Battery Modeling

Currently, the battery is still the most extensive energy storage device for providing and delivering electricity. There are many kinds of battery technology, such as lead-acid, NiCd, NiMH, or Li-ion. The characteristics of commercial batteries for HEV applications are shown in Table I [22]. For a lead-acid cell, the terminal voltage of battery V_b and the internal resistance R_b are strong functions of the state of charge (SOC). The battery actual voltage curve is not constant. This

is because the internal resistance is almost linear during the discharge, but the losses are substantially below 25% SOC due to the increase in the internal resistance.

Dynamic state model of the battery is necessary to develop a simulation model for the emulation of battery behavior. The model is developed from experimental cell data, where open circuit voltage (OCV) tests are performed on successive discharge of the battery, by the application of periodic current discharge. As for the temperature variation from 55°c to -30°c the OCV of a battery varies nonlinearly over the battery SOC. Therefore, the nonlinear RC models are developed to model nonlinear OCV characteristics of the battery.

TABLE I. CHARACTERISTICS OF COMMERCIAL BATTERIES FOR HEV APPLICATIONS

Battery Type		Capacity (Ah)	Voltage (V)	Resistance (mΩ)	W/kg % 95 eff	Usable SOC
NiMH	*Panasonic*	6.5	7.2	11.4	207	40%
	Ovonic	12	12	10	195	30%
	Saft	14	1.2	1.1	172	30%
Li-ion	*Saft*	12	4	7	256	20%
	Shin-kobe	4	4	3.4	745	18%
Lead-asid	*Panasonic*	25	12	7.8	77	28%

The proposed model consists of: 1) nonlinear voltage source *VOC(Z)* as a function of *SOC Z* to represent nonlinear characteristics of the *OCV*; 2) a capacitance *Cp* to model polarization effect; 3) a propagation resistor *Rb* to model propagation resistance; 4) a diffusion resistor *Rp* as a function of current *I*; and 5) an ohmic resistance *Rt* and terminal voltage *Vt* as shown in Fig. 2. The self-discharge resistor does not considered in the model because the self-discharge characteristic of the lithium battery is extremely low compared to other batteries such as nickel cadmium, lead-acid, nickel metal hydride type [34].

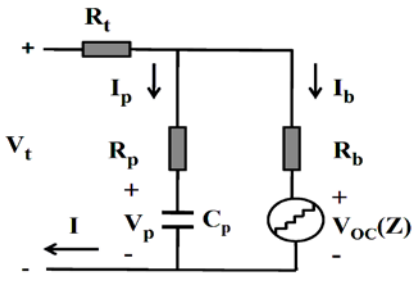

Fig. 2. Battery dynamic model structure

The voltage across the capacitance C_p is denoted as V_p. The terminal voltage equation is given as

$$V_t = IR_t + I_p R_p + V_p \quad (1)$$

$$V_t = IR_t + I_b R_b + V_{OC}(Z) \quad (2)$$

Where I is the instantaneous current (positive for charging, negative for discharging).

The SOC is defined as a ratio of the remaining capacity to the nominal capacity of the cell, where the remaining capacity is the number of ampere-hours that can be drawn from the cell at room temperature with the C/30 rate before it is fully discharged [34]. Based on this definition, the mathematical relation on the SOC is developed as

$$Z(t) = Z(0) + \int_0^t \frac{I_b(\tau)}{C_n} d\tau \quad (3)$$

Where Z(t) is SOC and C_n is the nominal capacitance of the cell which is defined as the number of ampere-hours that can be drawn from the cell at room temperature at the C/30 rate, starting with the cell fully charged [34].

B. Ultracapacitor Modeling

Ultracapacitors have the advantage of near-instantaneous energy delivery. The stored energy can be transferred to the dc-bus at nearly any discharge rate. In contrast, batteries will experience high internal losses if they are discharged too quickly. Thus ultracapacitors are of considerable interest for HEV applications.

The classical equivalent circuit of the UC unit is shown in Fig. 3. The model consists of a capacitance (*C*), an equivalent series resistance (ESR, *R*) representing the charging and discharging resistance, and an equivalent parallel resistance (EPR) representing the self-discharging losses [35]. The EPR models leakage effects and only impacts long-term energy storage performance of the UC.

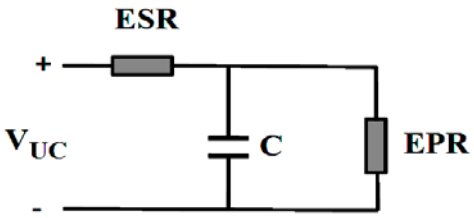

Fig. 3. Classical equivalent model for the UC unit

The voltage state of a UC (i.e., *RC* circuit) with a capacitance *C* draining charge into a resistance *R=ESR* may be described as

$$V(t) = V_i \exp(-\frac{t}{RC}) \quad (4)$$

The *RC* time constant determines the effective period of the charging and discharging processes for some initial voltage on the capacitor [35].

The ultracapacitor model is based on Maxwell Ultracapacitor's BMOD0058 15-V pack [36], which contains six 2.5-VBCAP0350 cells in series. The pack includes cell balancing and sturdy packaging. Since the acceptable motor-voltage range is chosen to be 250–400 V and the ultracapacitor pack will be connected directly to the high-voltage bus in the chosen topology, the maximum ultracapacitor pack voltage should be around 400 V. Thus, 27

packs are used in series so that the maximum ultracapacitor voltage is 405 V (although the control strategy will ensure that the voltage does not go above 400 V). Therefore, the optimization variable is chosen to be the number of strings in parallel. The ultracapacitor voltage is calculated using

$$V_{uc}(t) = V_{uc}(0) + \frac{1}{C}\int_0^t I_{uc}(\lambda)d\lambda \quad (5)$$

Where C is the total capacitance of ultracapacitor. The voltage drop and losses due to the internal resistance are also included.

C. Fuel Cells Modeling

A fuel cell is a galvanic cell in which the chemical energy of a fuel is converted directly into electrical energy by means of electrochemical processes. The chemical reaction in a fuel cell is similar to that in a chemical battery. The thermodynamic voltage of a fuel cell is closely associated with the energy released and the number of electrons transferred in the reaction [37].

The fuel cell is connected to the main dc-bus via a dc/dc converter and receives a power command from a system-level controller. The fuel cell model follows the slow evolution of the actual available power as it tries to respond to the command. This represents the slow dynamics between fuel input and electric power output. The dc/dc converter adjusts the current quickly to regulate the fuel cell voltage and deliver the available power. In a fuel cell, the fuel input is the physical parameter that is controlled. The steady-state electrical characteristics of a typical single PEM fuel cell are shown in Fig. 4. For any given fuel flow with a target voltage of 0.6 V/cell, there is a one-to-one mapping between output power and fuel input [38].

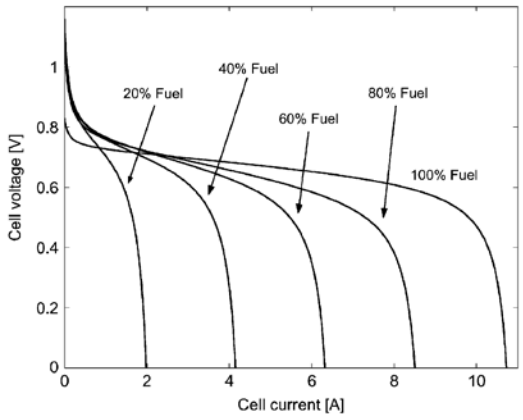

Fig. 4. The steady-state characteristics of a typical single PEM fuel cell

According to [39], the polarization curve for the PEMFC is obtained from the sum of the Nernst's voltage, the activation over voltage and the ohmic over voltage. Assuming constant temperature the FC output voltage may be expressed as

$$V_{cell} = E + \eta_{act} + \eta_{ohmic} \quad (6)$$

$$\eta_{act} = -B\ln(CI'_{FC}) \quad (7)$$

$$\eta_{ohmic} = -R^{\text{int}} I'_{FC} \quad (8)$$

The Nernst's instantaneous voltage may be expressed as

$$E = N_0\left[E_0 + \frac{RT}{2F}\log\left[\frac{p_{H_2}\sqrt{p_{O_2}}}{p_{H_2O}}\right]\right] \quad (9)$$

The FC model used in this paper is realized in MATLAB and Simulink. Then this model is embedded into the Sim-Power Systems of MATLAB as a controlled voltage source.

D. Buck-Boost Converter Modeling

The main objective is to establish the dynamic control strategy of the dc/dc converters for energy management between the batteries and ultracapacitors. This dynamic control strategy is based on current control because the dc-link voltage level is imposed by the battery module. The ultracapacitor module is connected to the dc link using a bidirectional converter to ensure the charge and discharge of the electric power storage devices. The converter control depends on the energy-management strategy between the hybrid sources and the hybrid vehicle energy request. This converter modeling includes the boost and buck operating modes [40].

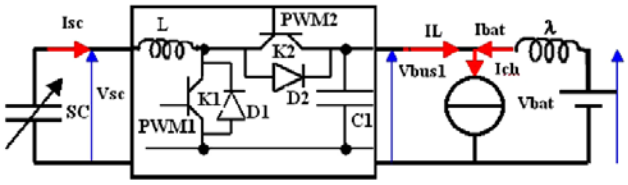

Fig. 5. Buck–boost converter topology

1) Boost Converter Modeling

During this operating mode, K_1 is on, and K_2 is off, and the ultracapacitor module provides energy to the dc bus. The I_{SC} ultracapacitor current direction is presented in Fig. 5, and the converter model is given by the following differential equations [40]:

$$V_L = L.\frac{d}{dt}(i_{SC}) = V_{SC} - (1-\alpha_1)V_{bus1} \quad (10)$$

$$I_{ch} = I_L + I_{bat} \quad (11)$$

$$V_\lambda = \lambda.\frac{d}{dt}(i_{bat}) = V_{bat} - V_{bus1} \quad (12)$$

2) B. Buck Converter Modeling

Contrary to boost mode, here, K_2 is on, and K_1 is off, and the ultracapacitor module is charged by a battery. The converter model is given by (13)-(15). The *I*sc and I_L currents have a direction opposite from that of the currents shown in Fig. 5. We have

$$V_L = L.\frac{d}{dt}(i_{SC}) = \alpha_2 V_{bus1} - V_{SC} \quad (13)$$

$$I_{bat} = I_L + I_{ch} \quad (14)$$

$$V_\lambda = \lambda.\frac{d}{dt}(i_{bat}) = V_{bat} - V_{bus1} \quad (15)$$

These average models present a nonlinear behavior of converters because of crosses between the control variables (i.e., α_1 and α_2) and the state variables (i.e., voltages and currents).

IV. Simulation Results and Analysis

Sample simulation results presented here focus on the dynamic behavior of currents and voltages in the system and the losses in the subsystems. The vehicle configuration combines the fuel cell with a battery and an ultracapacitor as the energy storage unit. All configurations are simulated over the duty cycle.

A. HEV with Batteries, Ultracapacitors and Fuel Cell

The batteries are the primary energy source of the vehicle and balance the power production and consumption in the system. The fuel cell setup consists of 65 fuel cell stacks in parallel, each having 70 single cells in series. Assuming that individual cells operate at 0.6 V with a maximum current of 8 A at 100% fuel input, the maximum available output power is 22 kW. The dc-dc converter is implemented with 24 parallel MOSFETs, each rated for 50 A, on the primary transformer side and with single power diodes on the secondary side. The transformer turns ratio is 48/300 and the series resistance of diode and MOSFET is 0.59Ω and 0.03Ω respectively. Turn on/off time constant is 30/15s. As ultracapacitors respond rapidly, lower capacity can be tolerated compared to batteries. A 3.2MJ ultracapacitor should be sufficient for the HEV requirements [34]. Assuming a maximum voltage of 300 V for the ultracapacitor, the required capacitance is 50 F. The ESR value of the capacitor is assumed to be 0.03Ω. A bidirectional dc/dc converter is used between ultracapacitor and dc-bus. The nominal battery voltage is 312V and its capacity is 28.26 MJ.

The behavior of the traction system and the fuel cell when combined with battery and an ultracapacitor are given in Fig. 6. It is consist of Vehicle speed; gear setting; the rotational speed of the induction motor; the actual induction motor torque and the dc-bus load current. Here shifting of gears is clearly visible in motor speed by short-term accelerations and decelerations and again is obvious as large spikes in the torque.

The time constants associated with the fuel cell are much slower than those of the traction system. Thus, the behavior of most of the fuel cell signals will be slower and closer to an average value.

Fig. 7 shows a collection of graphs from the HEV subsystems. The output current of the fuel cell stack going into the dc-dc converter, where the transients of this current are slow compared to the induction machine load current, giving an average of the required load current. Notice that the turn-on time of the fuel cell is considerably larger than the turn-off time, as defined in the fuel cell model. The evolution of the battery charge SOC and the ultracapacitor SOC during the drive cycle can also be seen in Fig. 7. It can be noticed that the ultracapacitor charge fluctuates more than the battery charge owing to its smaller capacity. Thus, with an ultracapacitor, the system is significantly more efficient.

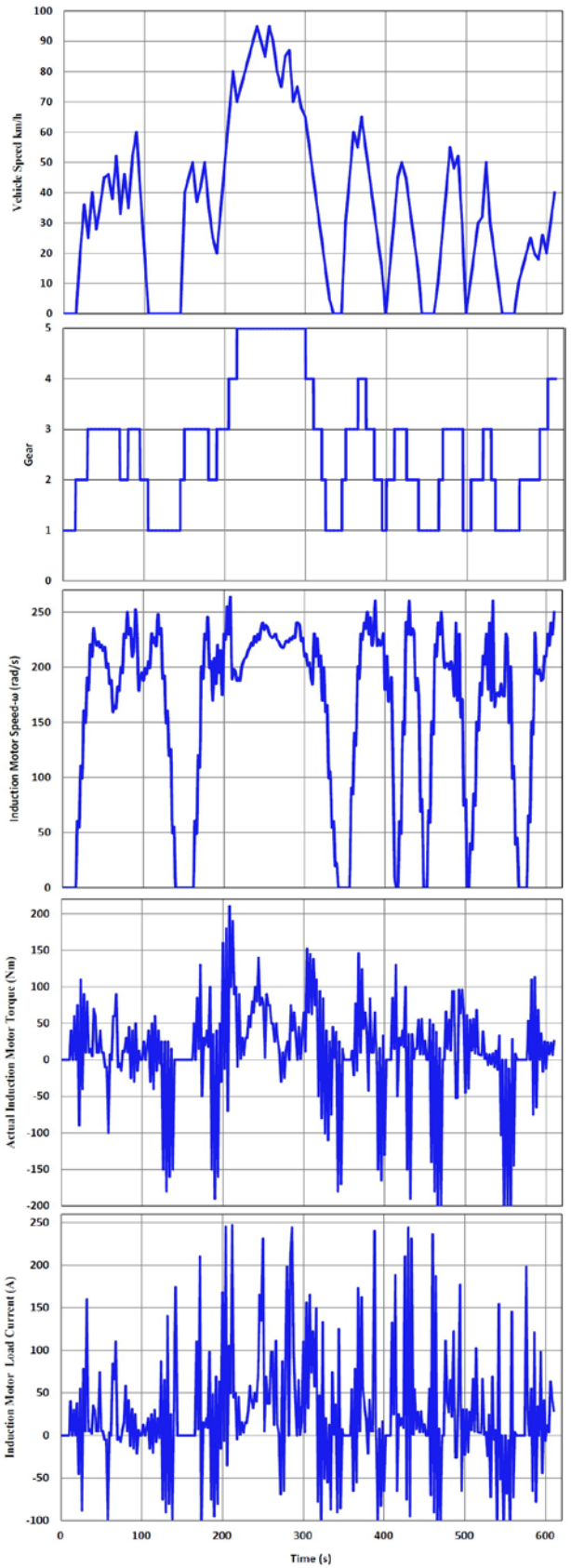

Fig. 6. Vehicle speed; gear setting; the induction motor speed; the actual induction motor torque and the dc-bus load current.

The battery capacity is larger than needed for this cycle, thus the short-term changes in the battery charge are only a few percent. Notice that the battery voltage range is narrow because the SOC is changing only slightly. However, the bus voltage drops significantly every time the vehicle accelerates and increases when the vehicle regenerates. This is related to battery resistance and the small bus capacitance. It is evident that the buck-boost converter between the ultracapacitor and the bus can enforce near-constant bus voltage.

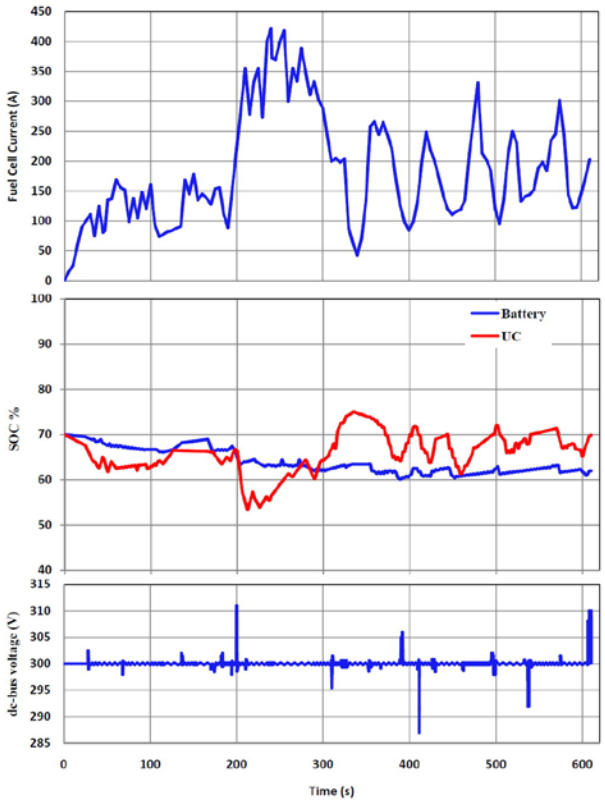

Fig. 7. Fuel Cell current; SOC of battery and UC; dc-bus voltage

Load or regeneration spikes translate into fast discharges of the battery and result in substantial loss. Although there is some uncertainty due to the low ultracapacitor ESR, the losses in the ultracapacitor module are more than an order of magnitude lower than in the battery module. But when power is cycled quickly, the battery experiences high losses, while the losses in the ultracapacitor are much lower.

The simulation can be checked with a power balance. The values of the average power production and consumption in the HEV with the fuel cell, battery and ultracapacitor are given in Table II.

TABLE II. POWER BALANCE OF HEV MODEL

	Battery	**UC**	**FC**	**Vehicle system**	**Total**
Power produced	1304 W	14.09 W	633 W	----	1937 W
Power consumed	715.5 W	117.2 W	49.3 W	1032 W	1914 W

Average power produced in the system must equal consumed average power plus any change in stored energy. The average power produced by the fuel cell for this test run is 633 W. The battery is discharged by 4.7%, corresponding to an average power of 1.304 kW. The 0.72% charge decrease in the ultracapacitor corresponds to an average power production of 14.1 W, resulting in a total average power production of 1.937 kW. The average power consumption of the traction system is 1.032 kW, and the average losses in the battery and the fuel cell dc-to-dc converter are 715.5 W and 49.3 W, respectively. The losses in the ultracapacitor module are 117.2 W, considerably lower than the battery losses. The total average power consumption is about 1.914 kW very close to the average power production. These results depend on achieving UCs with sufficiently low ESR.

The small difference between production and consumption is a computational limit. Uncertainties in the model and parameters are sources of errors when comparing the results with measured data. Some of the uncertainty factors in this simulation are the fuel cell model and its parameters. Other uncertainty factors are the battery parameters, which were approximated from actual measurements. The actual discharge function of the battery is slightly steeper than modeled, which decreases the output power and increases battery losses by a small margin.

V. CONCLUSION

Steady-state simulation tools for the design and analysis of hybrid electric automotives have been developed in recent. In the past, dynamic simulation models have focused mainly on the analysis of control strategies. The advantages of an FC hybrid vehicle could include improved vehicle performance and fuel economy and lower system cost. The degree of hybridization benefits from: 1) FC efficiency characteristics; 2) FC downsizing; 3) displacing FC tasks with the secondary source functionality; or 4) energy recovery through regenerative braking. This paper has studied the role of the energy-storage device in FC hybrid vehicles to understand their potential impact on dynamic performances. In this paper, a dynamic simulation system for an HEV, implemented in Matlab/Simulink, has been presented. The model features fuel cells as the vehicle's energy source, batteries and ultracapacitors as energy storage units, and an induction machine drive in the traction system. The purpose of the model is to provide an in-depth analysis of sublevel components in the vehicle and loss analysis in power electronics devices in converters associated with these sublevel components. In this paper, a dynamic model of a hybrid electric vehicle that includes fuel cells, batteries, ultracapacitors, and induction machine drives is presented. Simulation results of vehicle configuration are discussed. The focus of the model is a detailed assessment of different subsystem components.

REFERENCES

[1] Iqbal Husain, Electric and Hybrid Vehicles Design Fundamentals, (Taylor & Francis e-Library, 2005)

[2] S. Lukic, J. Cao, R. C. Bansal, F. Rodriguez, and A. Emadi, Energy storage systems for automotive applications, IEEE Trans. Ind. Electron., vol. 55, no. 6, Jun. 2008, pp. 2258–2267.

[3] C. C. Chan and Y. S. Wong, Electric vehicles charge forward, IEEE Pow. Ene. Mag., vol. 2, no. 6, Nov./Dec. 2004, pp. 24–33.

[4] D. Hoelscher, A. Skorez, Y. Gao, and M. Ehsani, Hybridized electric energy storage systems for hybrid electric vehicles, in Proc. IEEE Vehicle Power Propulsion Conf., Sep. 2006, pp. 1–6.

[5] A. Emadi, A. Khaligh, C. H. Rivetta and G. A. Williamson, Constant Power Loads and Negative Impedance Instability in Automotive Systems: Definition, Modeling, Stability, and Control of Power Electronic Converters and Motor Drives IEEE Trans. Veh. Technol., vol. 55, no. 4, JULY 2006.

[6] J. Moreno, M. E. Ortuzar, and J. W. Dixon, Energy management system for a hybrid electric vehicle, using ultracapacitors and neural networks,'' IEEE Trans. Ind. Electron., vol. 52, no. 2, Apr. 2006, pp. 614–623.

[7] C. Musardo, G. Rizzoni, and B. Staccia, A-ECMS: An adaptive algorithm for hybrid electric vehicle energy management, in Proc. IEEE CDC-ECC, Seville, Spain, Dec. 2005, pp. 1816–1823.

[8] Y. Gao and M. Ehsani, Parametric design of the traction motor and energy storage for series hybrid off-road and military vehicles, IEEE Trans. Power Electron., vol. 21, no. 3, May 2006, pp. 749–756.

[9] P. Atwood, S. Gurski, D. J. Nelson, and K. B. Wipke, Degree of hybridization modeling of a fuel cell hybrid electric sport utility vehicle, SAE Trans., J. Engines, vol. 110, SAE Paper 2001-01-0236, pp. 93–100.

[10] P. Thounthong, B. Davat, and S. Raël, Drive friendly, IEEE Power Energy Mag., vol. 6, no. 1, Jan./Feb. 2008, pp. 69–76.

[11] K. Rajashekara and et al, Hybrid fuel cell power in aircraft, IEEE Ind. Appl. Mag., vol. 14, no. 4, Jul./Aug. 2008, pp. 54–60.

[12] W. Gao, Performance comparison of a fuel cell-battery hybrid powertrain and a fuel cell–ultracapacitor hybrid powertrain, IEEE Trans. Veh. Technol., vol. 54, no. 3, May 2005, pp. 846–855.

[13] A. Rousseau, P. Sharer, and R. Ahluwalia, Energy storage requirements for fuel cell vehicles, presented at the SAE World Congr., Detroit, MI, 2004, Paper SAE 2004-01-1302.

[14] J. Schiffer, O. Bohlen, R. W. De Doncker, D. U. Sauer, and A. K. Young, Optimized energy management for fuel cell–supercap hybrid electric vehicles, in Proc. IEEE Veh. Power Propulsion Conf., Chicago, IL, 2005, pp. 341–348.

[15] Y. Wu and H. Gao, Optimization of fuel cell and supercapacitor for fuel-cell electric vehicles, IEEE Trans. Veh. Technol., vol. 55, no. 6, Nov. 2006, pp. 1748–1755.

[16] M.-J. Kim and H. Peng, Combined control/plant optimization of fuel cell hybrid vehicles, in Proc. Amer. Control Conf., Minneapolis, MN, 2006, pp. 496–501.

[17] G. Paganelli, Y. Guezennec, and F. Rizzoni, Optimizing control strategy for hybrid fuel cell vehicle, presented at the SAE World Congr., Detroit, MI, 2002, Paper SAE 2002-01-0102.

[18] R. Schupbach and J. Balda, The role of ultracapacitors in an energy storage unit for vehicle power management, in Proc. IEEE Veh. Technol. Conf., Orlando, FL, 2003, pp. 3236–3240.

[19] G. Pede, A. Iacobazzi, S. Passerini, A. Bobbio, and G. Botto, FC vehicle hybridisation: An affordable solution for an energy-efficient FC powered drive train, J. Power Sources, vol. 125, no. 2, Jan. 2004, pp. 280–291.

[20] H. Fathy, J. Reyer, P. Papalambros, and A. Ulsoy, On the coupling between the plant and controller optimization problems, in Proc. Control Conf., Arlington, VA, 2001, pp. 1864–1869.

[21] Jennifer Bauman and Mehrdad Kazerani, A Comparative Study of Fuel-Cell–Battery, Fuel-Cell–Ultracapacitor, and Fuel-Cell–Battery–Ultracapacitor Vehicles IEEE Trans. Veh. Technol., vol. 57, NO. 2, March 2008, pp. 760-769.

[22] A. Khaligh, and Z. Li, Battery, Ultracapacitor, Fuel Cell, and Hybrid Energy Storage Systems for Electric, Hybrid Electric, Fuel Cell, and Plug-In Hybrid Electric Vehicles: State of the Art IEEE Trans. Veh. Technol., vol. 59, NO. 6, July 2010.

[23] A. Khaligh, A. Miraoui, and D. Garret, Guest editorial: Special section on vehicular energy-storage systems, IEEE Trans. Veh. Technol., vol. 58, no. 8, Oct. 2009, pp. 3879–3881.

[24] O. Onar and A. Khaligh, Dynamic modeling and control of a cascaded active battery/ultra-capacitor based vehicular power system, in Proc. IEEE Vehicle Power Propulsion Conf., Sep. 2008, pp. 1–4.

[25] Z. Li, O. Onar, A. Khaligh, and E. Schaltz, Design, control, and power management of a battery/ultra-capacitor hybrid system for small electric vehicles, in Proc. SAE World Congr. Exh., Detroit, MI, Apr. 2009, doc. No. 2009-01-1387.

[26] B. G. Dobbs and P. L. Chapman, A multiple-input dc–dc converter topology, IEEE Power Electron. Lett., vol. 1, no. 1, Mar. 2003, pp. 6–9.

[27] J. Cao and A. Emadi, A new battery/ultra-capacitor hybrid energy storage system for electric, hybrid and plug-in hybrid electric vehicles, in Proc. IEEE Vehicle Power Propulsion Conf., Sep. 2009, pp. 941–946.

[28] P. Thounthong, V. Chunkag, P. Sethakul, Be. Davat, and M. Hinaje, Comparative Study of Fuel-Cell Vehicle Hybridization with Battery or Supercapacitor Storage Device IEEE Trans. Veh. Tech., vol. 58, NO. 8, Oct. 2008, pp. 3892-3904.

[29] P. Thounthong, B. Davat, S. Raël, and P. Sethakul, Fuel cell highpower applications, IEEE Ind. Electron. Mag., vol. 3, no. 1, Mar. 2009, pp. 32–46.

[30] F. Baalbergen, P. Bauer, and J. A. Ferreira, Energy storage and power management for typical 4Q-load, IEEE Trans. Ind. Electron., vol. 56, no. 5, May 2009, pp. 1485–1498.

[31] A. Khaligh, Realization of parasitics in stability of DC-DC converters loaded by constant power loads in advanced multiconverter automotive systems, IEEE Trans. Ind. Electron., vol. 55, no. 6, Jun. 2008, pp. 2295–2304.

[32] J. Lai and D. J. Nelson, Energy Management Power Converters in Hybrid Electric and Fuel Cell Vehicles Proceedings of the IEEE, Vol. 95, No. 4April 2007, pp. 766-777.

[33] I. Sadli, P. Thounthong, J. P. Martin, S. Raël, and B. Davat, Behaviour of a PEMFC supplying a low voltage static converter, J. Power Sources, vol. 156, no. 1, May 2006, pp. 119–125.

[34] Song Kim, Nonlinear State of Charge Estimator for Hybrid Electric Vehicle Battery IEEE Trans. Power Electron., vol. 23, No. 4, July 2008, pp. 2027-2034.

[35] M. Uzunoglu, and M. S. Alam, Dynamic Modeling, Design, and Simulation of a Combined PEM Fuel Cell and Ultracapacitor System for Stand-Alone Residential Applications IEEE Trans. On Energy Conv., vol. 21, No. 3, September 2006, pp. 767-775.

[36] Maxwell Ultracapacitors. Available at: http://www.maxwell.com

[37] M. Ehsani, Y. Geo and A. Emadi, Modern Electric, Hybrid Electric and Fuel Cell Vehicles Fundamentals, Theory and Design,(2nd Ed. Taylor and Francis Group: pp.391-397 © 2010)

[38] M. Amrhein and P. T. Krein, Dynamic Simulation for Analysis of Hybrid Electric Vehicle System and Subsystem Interactions, Including Power Electronics IEEE Trans. Veh. Tech., vol. 54, No. 3May 2005, pp. 825-836.

[39] M. Y. El-Sharkh, A. Rahman, M. S. Alam, P. C. Byrne, A. A. Sakla, and T. Thomas, A dynamic model for a stand-alone PEM fuel cell power plant for residential applications, J. Power Sources, vol. 138, no. 1–2, Nov. 2004, pp. 199–204.

[40] M. B. Camara, H. Gualous, F. Gustin, and Alain Berthon, Design and New Control of DC/DC Converters to Share Energy Between Supercapacitors and Batteries in Hybrid Vehicles IEEE Trans. on veh. tech., vol. 57, no. 5, Sep. 2008, pp. 2721-2735.